WARSAW UNIVERSITY OF TECHNOLOGY Index 351733
FACULTY OF CIVIL ENGINEERING
COMMITTEE FOR CIVIL AND WATER ENGINEERING
POLISH ACADEMY OF SCIENCES ISSN 1230-2945

DOI: 10.24425/ace.2024.149864

ARCHIVES OF CIVIL ENGINEERING

Vol. LXX ISSUE 2 2024

pp. 291 –308

Research paper

Design of flexural strengthening based on fib Bulletin 90

Renata Kotynia[1], Monika Kaszubska[2]

Abstract: This paper presents the analysis of intermediate and end debonding failure in slab strengthened using carbon tapes (Carbon Fiber Reinforced Polymer). The calculations are based on the more accurate method in the latest fib Bulletin 90. Consideration of additional effects based on three conditions: basic bond, bond friction and member curvature in the intermediate crack debonding analysis give the ratios $\Delta F_{fEd}/\Delta F_{fRd}$ from 0.01 to 0.11, depending on the cross-section. For comparison in the simplified analysis of the ratio, M_{Ed}/M_{Rd} is equal 0.76. It is clearly visible the methods requiring more computational effort give lower values of element effort and allows the design to be more economical. As the strengthening fulfills the ultimate limit state, it does not meet the serviceability limit state.

Keywords: externally bonded reinforcement (EBR), fiber reinforced polymer (FRP), flexure, strengthening, load capacity

[1]Prof., PhD., Eng., Lodz University of Technology, Department of Concrete Structures, Al. Politechniki 6, 93-590 Łódź, Poland, e-mail: renata.kotynia@p.lodz.pl, ORCID: 0000-0002-7247-1229

[2]PhD., Eng., Lodz University of Technology, Department of Building Materials Physics and Sustainable Construction, Al. Politechniki 6, 93-590 Łódź, Poland, e-mail: monika.dymecka@p.lodz.pl, ORCID: 0000-0002-9797-675X

1. Introduction

Reinforcement of reinforced concrete elements for bending with the use of composite tapes and mats is a commonly used method of increasing the bending load capacity of elements which, after changing the utility function of the object, show a load capacity deficiency. The need for reinforcement may also result from the creation of an additional concentrated or linear load on the floor. The most prevalent failure mode in concrete beams strengthened in flexure with externally applied FRP is loss of composite action due to debonding, typically after (and rarely before) steel yielding. Debonding occurs through the concrete according to one of the following failure modes: intermediate crack debonding, end debonding, or concrete cover separation. Intermediate crack debonding and end debonding develop when the bond strength is exceeded. However, they are different with respect to the starting point of the debonding process, so it should be distinguished into two areas: the end anchorage region and the rest of the member. The behavior of bond between FRP and concrete and hence both intermediate crack debonding and end debonding can be characterized based on the bond shear stress-shear slip relation. Concrete cover separation develops when a shear crack in the end region of the FRP propagates into a debonding mode at the level below the internal steel reinforcement [1].

For the analysis of intermediate crack debonding different levels of approximation are available in [1]: the simplified FRP stress limit method and a more accurate method. The simplified FRP stress limit method is based on the ultimate FRP strain that has been defined on the safe side. The more accurate method is based on determining the crack spacing and on checking the FRP force difference at an element between two adjacent cracks. The background of this method was formulated by Niedermeier [2] and developed by Neubauer [3]. The bearing capacity condition is met if the change in force in the strip in the element between cracks ΔF_{fEd} is lower than the bond strength of the strips to the concrete: ΔF_{fRd} on each section between the cracks: $\Delta F_{fEd} \leq \Delta F_{fRd}$. The member is divided into several sections by means of the flexural cracks ($x_{cr}, x_{cr} + s_r, \ldots$) and the increase of tensile forces in FRP strips on the sections between the cracks is calculated [1]:

$$\Delta F_{fEd} = F_{fEd}(x_{cr} + s_r) - F_{fEd}(x_{cr}) \tag{1.1}$$

The bond strength of the strips to the concrete ΔF_{fRd} is the sum of three effects: the force from the bilinear bond stress–slip relationship $\Delta F_{fk,B}$, the force from an additional frictional bond that occurs at the places where debonding has already taken place $\Delta F_{fk,F}$ and the component from curvature $\Delta F_{fk,C}$ [4–6], Fig. 1:

$$\Delta F_{fRd} = \frac{\Delta F_{fk,B} + \Delta F_{fk,F} + \Delta F_{fk,C}}{\gamma_{fb}} \tag{1.2}$$

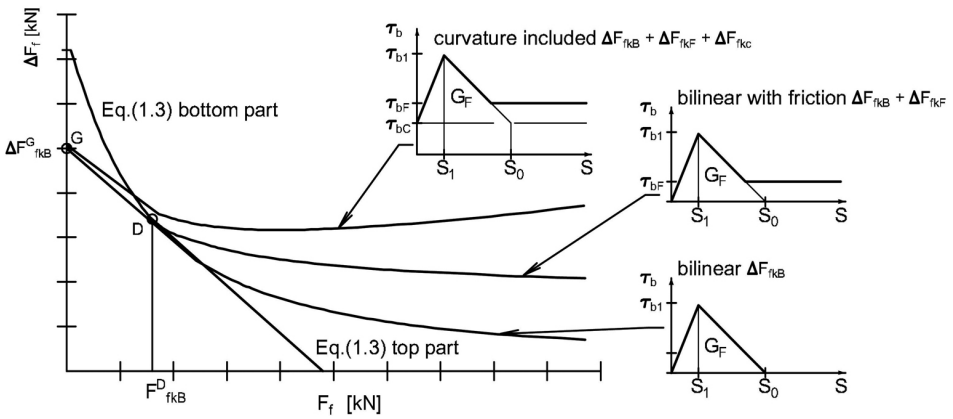

Fig. 1. FRP force due to basic bond, bond friction and member curvature

The change in force $\Delta F_{fk,B}$ is consisted from two parts:

$$\Delta F_{fk,B} = \begin{cases} \Delta F^G_{fk,B} - \dfrac{\Delta F^G_{fk,B} - \Delta F^D_{fk,B}}{\Delta F^D_{fk,B}} F_{fEd} & \text{for} \quad F_{fEd} \le F^D_{fk,B} \\ \sqrt{b_f^2 \tau_{b1k} s_{0k} E_f t_f + F^2_{fEd}} - F_{fEd} & \text{for } F^D_{fk,B} < F_{fEd} < F_{fd} \end{cases} \tag{1.3}$$

$$\Delta F^G_{fk,B} = f_{fbk}(s_r) b_f t_f \tag{1.4}$$

$$\Delta F^D_{fk,B} = \sqrt{b_f^2 \tau_{b1k} s_{0k} E_f t_f + {F^D_{fk,B}}^2} - F^D_{fk,B} \tag{1.5}$$

$$F^D_{fk,B} = \frac{s_{0k} E_f b_f t_f}{s_r} - \tau_{b1k} \frac{s_r b_f}{4} \tag{1.6}$$

The first represents the range over which the required transfer length of the bilinear bond stress–slip model is greater than the length of the element between cracks (s_r). The F_{fEd} force corresponds to the force in the composite at the location of the adjacent crack subjected to less stress and F_{fd} corresponds to the designed composite breaking load. Characteristic bond stresses as a function of crack spacing are:

$$f_{fbk}(s_r) = \begin{cases} \sqrt{\dfrac{E_f s_{0k} \tau_{b1k}}{t_f}} \dfrac{s_r}{l_e} \left(2 - \dfrac{s_r}{l_e}\right) & \text{for } s_r < l_e \\ \sqrt{\dfrac{E_f s_{0k} \tau_{b1k}}{t_f}} & \text{for } s_r \ge l_e \end{cases} \tag{1.7}$$

$$l_e = \frac{\pi}{2} \sqrt{\frac{E_f t_f s_{0k}}{\tau_{b1k}}} \tag{1.8}$$

$$\tau_{b1k} = 0,37 \sqrt{f_{cm} f_{\mathrm{ctm}}} \tag{1.9}$$

The second component $\Delta F_{fk,F}$ is equal:

$$\Delta F_{fk,F} = \begin{cases} 0 & \text{for} \quad F_{fEd} \le F^D_{fk,B} \\ \tau_{bFk} b_f \left[s_r - \dfrac{2 t_f E_f}{\tau_{b1k}} \left(\sqrt{\dfrac{\tau_{b1k} s_{0k}}{E_f t_f} + \dfrac{F^2_{fEd}}{b^2_f t^2_f E^2_f}} - \dfrac{F_{fEd}}{b_f t_f E_f} \right) \right] & \text{for } F^D_{fk,B} < F_{fEd} < F_{fd} \end{cases} \tag{1.10}$$

$$\tau_{bFk} = 10,8 \alpha_{cc} f_{cm}^{-0,89} \tag{1.11}$$

The third component $\Delta F_{fk,C}$ represents the curvature of the member that influences the bond of the surface-mounted reinforcement. A convex curvature, as caused by deflection, causes a change in direction at each concrete element between cracks, which therefore leads to self-induced contact pressure. This contact pressure on the surface-mounted reinforcement brings an increase in bond strength. The empirical coefficient $\kappa_k = 24.3 \times 10^3$ N/mm considers the influence of the curvature on the bond [6]:

$$\Delta F_{fk,C} = s_r \kappa_k \frac{\varepsilon_f - \varepsilon_c}{h} b_f \tag{1.12}$$

The end debonding analysis for interfacial debonding can be conducted on the basis of the FRP anchorage capacity and two approaches are presented in [1]. In the first, the FRP curtailment point is determined following a similar methodology as for curtailment of internal steel reinforcement according to [7]. In the second the end debonding analysis is conducted at the flexural crack closest to the point of zero moment or at an arbitrary concrete element between cracks. The analysis at the flexural crack closest to the point of zero moment represents the standard situation. Crack develops at the point where the bending moment equals the cracking moment M_{cr}. In this point the applied moment M_{Ed} shall be smaller than the moment resistance $M_{Rd}(l_b)$, with the shift of the tension envelope, $M_{Ed} \le M_{Rd}(l_b)$. The prestrain of the reinforcement due to the load during strengthening shall not be considered in this analysis.

$$M_{Rd}(l_b) = \frac{\varepsilon^a_{fRk}(l_b) E_f}{\gamma_{fb}} A_f z^a_f + \frac{\varepsilon^a_{sRk}(l_b) E_s}{\gamma_s} A_s \tag{1.13}$$

The analysis of an arbitrary element between cracks is similar to the more accurate method in the analysis of intermediate crack debonding. The acting FRP force F_{fEd} should be lower than the resisting FRP force F_{fbd}, $F_{fEd} \le F_{fbd}$. The resisting FRP force is:

$$F_{fbd} = b_f t_f f_{fbd}(s_r) \tag{1.14}$$

$$f_{fbd}(s_r) = \frac{k_k}{\gamma_{fb}} k_b \beta_1 \sqrt{\frac{2E_f}{t_f} f^{2/3}_{cm}} \tag{1.15}$$

Moreover, considering the shift rule in this analysis, it has to be ensured that the cross-section between the support and the element between cracks being considered possesses sufficient load-carrying capacity even without the FRP.

The general equations of the methods used in the paper are presented above. Intermediate parameters and explanations of variables can be found in the further part of the article. The example in this article presents the analysis of intermediate and end debonding failure in slab strengthened using carbon tapes (Carbon Fiber Reinforced Polymer – CFRP). The calculations are based on the more accurate method published in Fib Bulletin 90 [1].

2. The case study

In the example, the geometry and load condition are used from the real structure. The slab is located in the residential building in which a wall is required to be constructed over the first-floor level. The slab is uniformly loaded and simply supported. The slab is not subject wet environment, the loads are static. The slab can be considered as a simply supported member over $L = 5.9$ m span. The bottom reinforcement of the slab consists of 6 steel bars with diameter $\emptyset = 16$ mm, the top reinforcement consists of 4 bars diameter $\emptyset = 8$ mm. The mechanical, geometrical characteristics and material properties are: concrete cover – $c = 27$ mm; slab's height – $h = 185$ mm; tensile bars: – $A_{s1} = 6$, $\emptyset 16 = 1206$ mm ^{2}; compressive bars – $A_{s2} = 4$, $\emptyset 8 = 201$ mm ^{2}; location of bottom and top reinforcement – $a_{s1} = 27 + \emptyset/2 = 35$ mm; $a_{s2} = 31$ mm; $d = 185 - 35 = 150$ mm; depth of bearing – $t = 200$ mm; location of the strip end – $a_{L,t} = 250$ mm; concrete C35/45, characteristic cylinder compressive strength – $f_{ck} = 35$ MPa; design compressive strength – $f_{cd} = \alpha f_{ck}/\gamma_c = 1 \cdot 35/1.5 = 23.3$ MPa ($\alpha = 1$); characteristic tensile strength – $f_{\text{ctm}} = 3.2$ MPa; $f_{ctk} = 0.7 \cdot f_{\text{ctm}} = 0.7 \cdot 3.2 = 2.2$ MPa; elastic modulus – $E_c = 34000$ MPa; steel reinforcement S400, elastic modulus – $E_s = 200000$ MPa; characteristic yielding strength – $f_{yk} = 400$ MPa; design strength – $f_{yd} = f_{yk}/\gamma_s = 400/1.15 = 348$ MPa; strengthening properties, characteristic tensile strength – $f_{fk} = 2500$ MPa; design tensile strength – ($\eta = 1$) $f_{fd} = \eta f_{fk}/\gamma_f = 2500/1.25 = 2000$ MPa; modulus – $E_f = 160000$ MPa; ultimate strain – $\varepsilon_{fud} = f_{fk}/\gamma_f/E_f = 2500/1.25/160000 = 12.5‰$; material factors – $\gamma_f = 1.25$, $\gamma_{fb} = 1.50$; thickness – $t_f = 1.2$ mm, width $b_{f1} = 100$ mm, strip spacing $s_f < 2h = 370$ mm. The assumed stress-strain relationships for the materials used in the calculations are identical to those in [1, 7]. The acting load consists of uniformly distributed permanent and live loads equal to (for the width of 1 m) $G_{1k} = 6.41$ kN/m^2 and $Q_{1k} = 2.00$ kN/m^2, respectively. Moreover, the slab is loaded of 3 m height wall $G_{2k} = 5.70$ kN/m. It was assumed that 41% of the wall's load will be taken by the slab of 1 m width acting zone $\approx$ width of wall +2 slab thickness + span/3 = 2.43 m (1/2.43 = 0.41). The characteristics bending moment: $M_{Ek} = 43.85$ kN·m. The combination for the ultimate limit state was obtained according to formula 6.10a [8]. Taking into account: $\gamma_{G,\text{sup}} = 1,35$, $\gamma_{G,\text{inf}} = 1.00$, $\gamma_{Q,1} = 1.50$, $\xi = 0.85$, $\psi_{0,1} = 0.7$, it is obtained for the ultimate limit state (ULS):

(6.10a) $1.35(G_{1k} + 0.41G_{2k}) + 1.5 \cdot 0.7Q_{1k} = 13.91$ kN/m

(6.10b) $0.85 \cdot 1.35(G_{1k} + 0.41G_{2k}) + 1.5Q_{1k} = 13.04$ kN/m

$$\text{SLS}: M_{Ek} = \frac{G_{1k} \cdot L^2}{8} + \frac{Q_{1k} \cdot L^2}{8} + \frac{0.41G_{2k} \cdot L^2}{8} = 43.87\ [\text{kN} \cdot \text{m}] \tag{2.1}$$

$$\text{ULS}: M_{Ed} = \frac{G_{1d} \cdot L^2}{8} + \frac{Q_{1d} \cdot L^2}{8} + \frac{0.41 G_{2d} \cdot L^2}{8} = 60.52 \text{ [kN} \cdot \text{m]} \tag{2.2}$$

To the cross-section analysis, it is made the following assumptions: the yielding of the bottom reinforcement ($\sigma_{s1} = f_{yd}$) and the strain in the concrete $\varepsilon_{cu} = 3.5‰$. The stress in the top reinforcement is equal to:

$$\sigma_{s2} = E_s \varepsilon_{s20} = E_s \varepsilon_{cu} \frac{x - a_{s2}}{x} < f_{yd} \tag{2.3}$$

Considering RC rectangular cross-section and the parabola-rectangle constitutive relationship for the concrete, the equilibrium of internal axial forces gives:

$$0.8095 b f_{cd} x + A_{s2} E_s \varepsilon_{cu} \frac{x - a_{s2}}{x} - A_{s1} f_{yd} = 0 \tag{2.4}$$

The above equation can be transform to quadratic equation in form $Ax^2 + Bx + C = 0$. It gives the depth of the neutral axis and then the strain in the steel reinforcement to verification earlier assumption:

$$0.8095 b f_{cd} x^2 + [A_{s2} E_s \varepsilon_{cu} - A_{s1} f_{yd}] x - A_{s2} E_s \varepsilon_{cu} a_{s2} = 0 \tag{2.5}$$

$$A = 0.8095 b f_{cd} \tag{2.6}$$

$$B = A_{s2} E_s \varepsilon_{cu} - A_{s1} f_{yd} \tag{2.7}$$

$$C = -A_{s2} E_s \varepsilon_{cu} a_{s2} \tag{2.8}$$

$$\Delta = B^2 - 4AC \tag{2.9}$$

$$x = \frac{-B + \sqrt{\Delta}}{2A} = 24.3 \text{ [mm]} \tag{2.10}$$

$$\varepsilon_{s10} = -\varepsilon_{cu} \frac{d - x}{x} = -18.12‰ \quad |\varepsilon_{s1}| > \varepsilon_{yd} = 1.74 \tag{2.11}$$

$$\varepsilon_{s20} = \varepsilon_{cu} \frac{x - a_{s2}}{x} = -0.97‰ \quad |\varepsilon_{s2}| < \varepsilon_{yd} = 1.74 \tag{2.12}$$

$$M_{Rd} = 0.8095 x b f_{cd} (d - 0.4159x) + A_{s2} E_s \varepsilon_{s20} (d - a_{s2}) = 59.52 \text{ [kN} \cdot \text{m/m]} \tag{2.13}$$

For further calculations the calculated bending moment is assumed according to the formula 6.10a: $M_{Ed} = 60.52$ kN·m $> M_{Rd} = 59.52$ kN·m, so the slab needs strengthening.

The first step is to determine the cracks spacing. The cracking moment is equal (assuming $f_{\text{ctm,surf}} = f_{\text{ctm}}$, $W_{c,0} = 5704166.67$ mm^3):

$$\kappa_{fl} = \max\left(1.6 - \frac{h}{1000}; 1.0\right) = \max\left(1.6 - \frac{185}{1000}; 1.0\right) = 1.42 \tag{2.14}$$

$$M_{cr} = \kappa_{fl} f_{\text{ctm,surf}} W_{c,0} = 1.42 \cdot 3.21 \cdot 5704166/10^6 = 25.91 \text{ [kN} \cdot \text{m]} \tag{2.15}$$

Because $M_{Ek} = 43.85$ kN·m $> M_{cr} = 25.91$ kN·m, slab is cracking. In this example, 3 CFRP strips per 1m (with spacing: $s_f = 333$ mm) with thickness; $t_f = 1.2$ mm and width $b_{f1} = 100$ mm are used. The mean bond stress in the reinforcing bars depends on the type of bar used. For ribbed rebars and good bond conditions ($\kappa_{vb1} = 1$):

$$f_{bsm} = \kappa_{vb1} \cdot 0.43 f_{cm}^{2/3} = 1 \cdot 0.43 \cdot 43^{2/3} = 5.28 \text{ [MPa]} \tag{2.16}$$

The mean bond force is determined via the circumference of the reinforcing steel and the mean bond stress:

$$F_{bsm} = \sum_{i=1}^{n} n_{s,i}\phi_{s,i}\pi f_{bsm} = 6 \cdot 16 \cdot \pi \cdot 5.28 = 1591.73 \text{ [N/mm]} \tag{2.17}$$

The transmission length of the reinforcing steel is ($z_s \approx 0.85h$):

$$l_{e,0} = \frac{M_{cr}}{z_s F_{bsm}} = \frac{25.91 \cdot 10^6}{0.85 \cdot 185 \cdot 1591.73} = 103.51 \text{ [mm]} \tag{2.18}$$

The formation of cracks in a strengthened reinforced concrete beam depends on many factors and indicates considerable scatter. A simplified approximation on the safe side is to assume it is 1.5 times the transmission length of the reinforcing steel:

$$s_r = 1.5 l_{e,0} = 1.5 \cdot 103.51 = 155.27 \text{ [mm]} \tag{2.19}$$

2.1. Design calculations for ultimate limit state (ULS) with passive CFPR laminates

2.1.1. Intermediate crack debonding

Due to the symmetry of the element, the calculations were made for half of the slab span. The element was divided in the length section s_r (Fig. 3), representing elements between cracks, starting at the maximum moment. After determining the location of cracks along the length of the element, determined the tensile force from external loads at the location of each crack based on the conditions of equilibrium of forces in the section (Fig. 2).

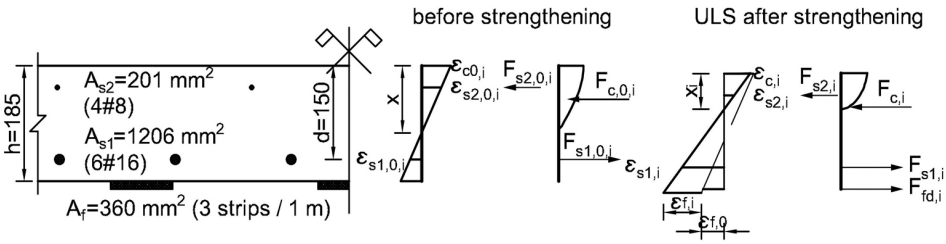

Fig. 2. Strain, stress and forces in RC slab strengthened with CFRP laminates

The bending moment at cracks before and after strengthening, load $p_0 = 6.41$ kN/m (assumed only permanent loads), $p = 13.91$ kN/m (according formula 6.10a [8]) determined based on:

$$M_{E0,i} = \frac{p_0 l}{2} x_{cr,i} - \frac{p_0 x_{cr,i}^2}{2} \tag{2.20}$$

$$M_{Ed,i} = \frac{pl}{2} x_{cr,i} - \frac{p x_{cr,i}^2}{2} \tag{2.21}$$

The strains ($\varepsilon_{c,0,i}$, $\varepsilon_{s1,0,i}$, $\varepsilon_{s2,0,i}$) before strengthening in the place of crack formation was determined by the iteration method, using the equations below:

$$F_{s1,0,i} = F_{c,0,i} + F_{s2,0,i} \tag{2.22}$$

$$F_{s1,0,i} = \frac{M_{E0,i}}{z_s} = \frac{M_{E0,i}}{0.85h} \tag{2.23}$$

$$F_{s2,0,i} = A_{s2} E_s \varepsilon_{s2,0,i} \tag{2.24}$$

$$\varepsilon_{s2,0,i} = -\varepsilon_{s1,0,i} \frac{\left(\dfrac{-\varepsilon_{c,0,i} d}{-\varepsilon_{c,0,i} + \varepsilon_{s1,0,i}} - a_{s2} \right)}{\left(d - \dfrac{-\varepsilon_{c,0,i} d}{-\varepsilon_{c,0,i} + \varepsilon_{s1,0,i}} \right)} \tag{2.25}$$

$$\varepsilon_{s1,0,i} = \frac{F_{s1,0,i}}{A_{s1} E_s} \tag{2.26}$$

$$F_{c,0,i} = k_1 f_{cd} b x_{0,i} \tag{2.27}$$

$$k_{1,0,i} = \begin{cases} 1000 \varepsilon_{c,0,i} \left(0,5 - \dfrac{1000}{12} \varepsilon_{c,0,i} \right) & \text{for} \quad \varepsilon_{c,0,i} \le 0.002 \\ 1 - \dfrac{2}{3000 \varepsilon_{c,0,i}} & \text{for } 0.002 < \varepsilon_{c,0,i} \le 0.0035 \end{cases} \tag{2.28}$$

In general, the considered slab is cracked already for permanent load without wall ($M_{G1d} = 37.65$ kN·m/m $> M_{cr}$ and $M_{G1k} = 27.89$ kN·m/m $> M_{cr}$). According to [1] the prestrain ($\varepsilon_{f,0,i}$ at the level of strips) is considered. Based on the equilibrium equations of moments and forces in the section, the strains $\varepsilon_{c,i}$ in concrete and $\varepsilon_{f,i}$ in CFRP strips and the height of the compressed concrete zone were determined for the sections after strengthening using the iteration method:

$$F_{s1,i} + F_{fd,i} = -F_{c,i} - F_{s2,i} \tag{2.29}$$

$$F_{s1,i}(d - k_2 x_i) + F_{fd,i}(h - k_{2,i} x_i) - F_{s2,i}(k_{2,i} x_i - a_2) = M_{Ed,i}(x_{cr,i} + a_L) \tag{2.30}$$

$$F_{s1,i} = \min \left(A_{s1} E_s \varepsilon_{s1,i}; f_{yd} A_{s1} \right) \tag{2.31}$$

$$F_{s2,i} = \min \left(A_{s2} E_s \varepsilon_{s2,i}; f_{yd} A_{s2} \right) \tag{2.32}$$

$$F_{fd,i} = A_f E_f \varepsilon_{f,i} \tag{2.33}$$

$$F_{c,i} = k_{1,i} f_{cd} b x_i \tag{2.34}$$

$$\varepsilon_{s1,i} = \frac{-\varepsilon_{c,i}(d - x_i)}{x_i} \tag{2.35}$$

$$\varepsilon_{s2,i} = -\varepsilon_{s1,i}(x_i - a_{s2})/(d - x_i) \tag{2.36}$$

$$k_{1,i} = \begin{cases} 1000 \varepsilon_{c,i} \left(0.5 - \dfrac{1000}{12} \varepsilon_{c,i} \right) & \text{for} \quad \varepsilon_{c,i} \le 0.002 \\ 1 - \dfrac{2}{3000 \varepsilon_{c,i}} & \text{for } 0.002 < \varepsilon_{c,i} \le 0.0035 \end{cases} \tag{2.37}$$

$$k_{2,i} = \begin{cases} \dfrac{8 - 1000\varepsilon_{c,i}}{4(6 - 1000\varepsilon_{c,i})} & \text{for} \quad \varepsilon_{c,i} \le 0.002 \\ \dfrac{1000\varepsilon_{c,i}(3000\varepsilon_{c,i} - 4) + 2}{2000\varepsilon_{c,i}(3000\varepsilon_{c,i} - 2)} & \text{for } 0.002 < \varepsilon_{c,i} \le 0.0035 \end{cases} \tag{2.38}$$

$$x_i = \frac{-\varepsilon_{c,i} h}{-\varepsilon_{c,i} + \varepsilon_{f,i} + \varepsilon_{f,0,i}} \tag{2.39}$$

The force obtained from iterations for each section are shown in Fig. 3.

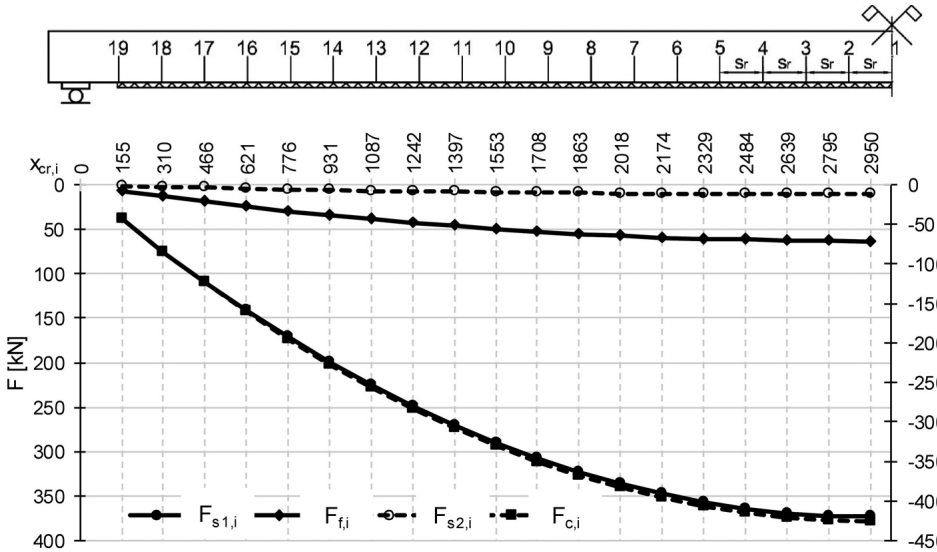

Fig. 3. Force in the place of crack formation (results of iterations)

The results of calculations made based on the forces equilibrium in the cross-section at the place of formation of cracks before and after strengthening allowed to determine the change in the tensile force ΔF_{fEd} between successive cracks ($F_{fEd,i} = F_{f,i}$). Following calculation of the bond strength is carried out for every concrete element between cracks. First some key parameters were determined. The parameters in the bilinear bond law are taken as characteristic values [1], $s_0 = 0.20$ mm and

$$\tau_{b1k} = 0.37\sqrt{f_{cm} f_{\text{ctm}}} = 0.37\sqrt{43 \cdot 3.21} = 4.35 \text{ [MPa]} \tag{2.40}$$

The effective bond length l_e is obtained as:

$$l_e = \frac{\pi}{2}\sqrt{\frac{E_f t_f s_{0k}}{\tau_{b1k}}} = \frac{\pi}{2}\sqrt{\frac{160000 \cdot 1.20 \cdot 0.20}{4.35}} = 147.64 \text{ mm} \tag{2.41}$$

Characteristic bond stresses as a function of crack spacing $s_r = 155.27$ mm > l_e):

$$f_{fbk}(s_r) = \sqrt{\frac{E_f s_{0k} \tau_{b1k}}{t_f}} = \sqrt{\frac{160000 \cdot 0.20 \cdot 4.35}{1.20}} = 340.47 \text{ [MPa]} \tag{2.42}$$

The component parameters are:

$$\Delta F^{G}_{fk,B} = f_{fbk}(s_r) b_f t_f = 340.47 \cdot 100 \cdot 3 \cdot 1.20/1000 = 122.57 \text{ [kN]} \tag{2.43}$$

$$F^{D}_{fk,B} = \frac{s_{0k} E_f b_f t_f}{s_r} - \tau_{b1k} \frac{s_r b_f}{4} = \left(\frac{0.20 \cdot 160000 \cdot 100 \cdot 3 \cdot 1.2}{155.27} - 4.35 \frac{155.27 \cdot 100 \cdot 3}{4} \right) /1000 = 23.57 \text{ [kN]} \tag{2.44}$$

$$\Delta F^{D}_{fk,B} = \sqrt{b_f^2 \tau_{b1k} s_{0k} E_f t_f + {F^{D}_{fk,B}}^2} - F^{D}_{fk,B} = \sqrt{(300^2 \cdot 4.35 \cdot 0.20 \cdot 160000 \cdot 1.2)/10^6 + 23.57^2} - 23.57 = 101.24 \text{ [kN]} \tag{2.45}$$

$$\tau_{bFk} = 10.8 \alpha_{cc} f_{cm}^{-0,89} = 10.8 \cdot 43 \cdot 0.85 = 0.32 \text{ [MPa]} \tag{2.46}$$

The design tensile force in FRP is equal $F_{fd} = 240.00$ kN. The force from the bilinear bond stress–slip relationship $\Delta F_{fk,B}$ and the force from an additional frictional bond that occurs at the places where debonding has already taken place $\Delta F_{fk,F}$ are calculated according to Eq. (1.10). The component from curvature $\Delta F_{fk,C}$ is calculated according to Eq.(1.12). The results for all sections are summarized in Fig. 4. In all sections the condition: $\Delta F_{fEd} \leq \Delta F_{fRd}$ is fulfilled.

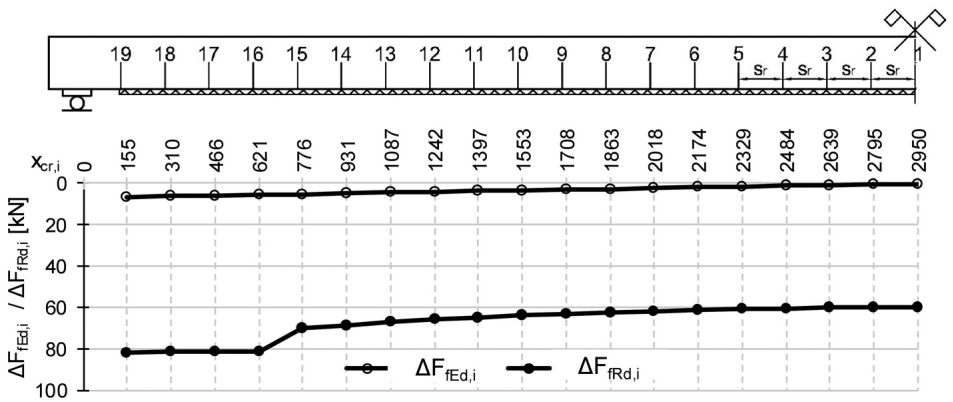

Fig. 4. The comparison ΔF_{fEd} and ΔF_{fRd}

2.1.2. End debonding

The location of the flexural crack closest to the point of zero moment shall be obtained under the design loads in the ultimate limit state and without considering the shift of the tension envelope. The position of the first flexural crack is gained equating $M_{Ed}(x_{cr}) = M_{cr}$. Finally, for further analysis was assumed $x_{cr} = 719.11$ mm. The tensile force in the FRP can be anchored, along the bond length, through bond between the FRP and the concrete. The anchorage length of the strip is the distance between the cross-section considered and the end of the FRP strip (the distance of the straps from the support $a_f = 50$ mm, support

width 200 mm):

$$l_b = x_{cr} - \frac{t}{2} - a_f = 719.11 - \frac{200}{2} - 50 = 569.11 \text{ [mm]} \tag{2.47}$$

The applied moment $M_{Ed} = 60.52$ kN·m for $p = 13.91$ kN/m and section $x_{cr} + a_L$) at the flexural crack closest to the point of zero moment is obtained by taking into account the shift rule, according to [7] ($a_L = d = 150$ mm). The limit strain in the strips $\varepsilon^a_{fRk,\lim}$ can be estimated for characteristic maximum bond strength of the FRP, using $\beta_1(l_b) = 1$, so $f_{fbk} = 340.47$ MPa. The maximum bond length (the effective bond length l_e (for 5% characteristic value)) and the corresponding anchorage length are calculated:

$$k_b = \max\left\{\begin{array}{c}\sqrt{\dfrac{2 - b_f/b}{1 + b_f/b}} \\ 1\end{array}\right. = \max\left\{\begin{array}{c}\sqrt{\dfrac{2 - 300/100}{1 + 300/100}} \\ 1\end{array}\right. = 1.14 \tag{2.48}$$

$$l_e \approx 1.5\frac{\pi}{k_b}\sqrt{\frac{E_f t_f}{8 f_{cm}^{\frac{2}{3}}}} = 1.5\frac{\pi}{1.14}\sqrt{\frac{160000 \cdot 1.20}{8 \cdot 43^{\frac{2}{3}}}} = 182.22 \text{ mm} \tag{2.49}$$

$$l_{b,\lim} = 164.00 \text{ mm} \tag{2.50}$$

FRP strip's strain at the flexural crack closest to the point of zero moment is obtained as ($l_b > l_{b,\lim}$):

$$\varepsilon^a_{fRk,\lim} \approx \frac{f_{fbk}}{E_f} \approx \frac{340.47}{160000} = 0.0021 \tag{2.51}$$

$$\varepsilon^a_{fRk}(l_b) = \left\{\begin{array}{ll}\sin\left(\dfrac{\pi}{2}\dfrac{l_b}{l_{b,\lim}}\right)\varepsilon^a_{fRk,\lim} & \text{for } 0 < l_b < l_{b,\lim} \\ \varepsilon^a_{fRk,\lim} & \text{for } \quad l_b \geq l_{b,\lim}\end{array}\right. = \varepsilon^a_{fRk,\lim} = 0.0021 \tag{2.52}$$

The depth of the compression zone at the flexural crack closest to the point of zero moment is calculated through cross section analysis. The depth of the compression zone is $x^a = 51.14$ mm. The slippage of the FRP strip is given as follows ($l_b > l_{b,\lim}$):

$$s^a_r(l_b) = \left\{\begin{array}{ll}0.213\left[1 - \cos\left(\dfrac{\pi}{2}\dfrac{l_b}{l_{b,\lim}}\right)\right] & \text{for } \quad 0 < l_b < l_{b,\lim} \\ 0.213 + \left(l_b - l_{b,\lim}\right)\varepsilon^a_{fRk,\lim} & \text{for } \quad l_b \geq l_{b,\lim}\end{array}\right. = \tag{2.53}$$

$$0.213 + \left(l_b - l_{b,\lim}\right)\varepsilon^a_{fRk,\lim} = 0.213 + (569.11 - 164.00) \cdot 0.0021 = 1.08$$

The bond coefficient for steel reinforcement is obtained by means (with the bond coefficients are $\kappa_{b1k} = 2.545$, $\kappa_{b2} = 1.0$, $\kappa_{b3} = 0.8$ and $\kappa_{b4} = 0.2$ for ribbed bars):

$$\kappa_{bsk} = \kappa_{b1k}\sqrt{\frac{f_{cm}^{\kappa_{b2}}}{E_s \Phi_s^{\kappa_{b3}} \left(E_f t_f\right)^{\kappa_{b4}}}} = \tag{2.54}$$

$$2.545 \cdot \sqrt{\frac{43^1}{200000 \cdot 16^{0.8} \left(160000 \cdot 1.20\right)^{0.2}}} = 0.0036$$

The strain of the steel reinforcement is calculated as (where $a_N = 0.25$ for ribbed steel reinforcement, $\kappa_{vb} = 1$ for good bond conditions, the effective depth of steel reinforcement $d_s^a = d = 150$ mm, the effective depth of FRP reinforcement $d_f^a = h = 185$ mm, the depth of the compression zone $x^a = 51.14$ mm, the internal lever arms for the FRP $z_f^a = 166.21$ mm and for the steel reinforcement $z_s^a = 131.21$ mm):

$$\varepsilon_{sRk}^a(l_b) = \min\left(\kappa_{vb}\kappa_{bsk}\left[s_r^a(l_b)\right]^{(a_N+1)/2}\left(\frac{d_s^a - x^a}{d_f^a - x^a}\right)^{(a_N+1)/2}; \frac{f_{yk}}{E_s}\right) = \min(0.00312; 0.0020) = 0.0020 \tag{2.55}$$

The moment resistance is calculated according to: $M_{Rd}(l_b) = 68.64$ kN·m $> M_{Ed} = 30.41$ kN·m. The second option analysis of end debonding is the analysis at an arbitrary element between cracks. It may be necessary for those members in which owing to the low tensile strength of the concrete the flexural crack closest to the point of zero moment is close to the support. In the considered example, such a situation does not occur (above analysis). In this analysis, the position of the considered element between the cracks can be assumed at the end of the strips, and its length is equal to the crack spacing $s_r = 155.27$ mm. The distance of the straps from the support $a_f = 50$ mm, support width 200 mm. Thus, the cross-section under consideration is $x_{cr} = 305.27$ mm from the center of the support. To determine the parameter β_1, the length of the anchorage is equal to the crack spacing, $l_b = s_r = 155.27$ mm:

$$\beta_1 = \begin{cases} \frac{l_b}{l_e}\left(2 - \frac{l_b}{l_e}\right) < 1 & \text{for } l_b < l_e \\ 1 & \text{for } l_b \geq l_e \end{cases} = \min\left[\frac{155.27}{182.22}\left(2 - \frac{155.27}{182.22}\right); 1\right] = 0.98 \tag{2.56}$$

The design bond strength as a function of the crack spacing is:

$$f_{fbd}(s_r) = \frac{k_k}{\gamma_{fb}} k_b \beta_1 \sqrt{\frac{2E_f}{t_f} f_{cm}^{2/3}} = \frac{0.17}{1.50} \cdot 1.14 \cdot 0.98 \cdot \sqrt{\frac{2 \cdot 160000}{1.20} 43^{2/3}} = 229.34 \text{ [MPa]} \tag{2.57}$$

The resisting FRP force is:

$$F_{fbd} = b_f t_f f_{fbd}(s_r) = 300 \cdot 1.20 \cdot 229.34/1000 = 82.56 \text{ [kN]} \tag{2.58}$$

The tensile force in CFRP strips is less than the load capacity, $F_{fEd} = 16.36$ kN $< F_{fbd} = 82.56$ kN. The resistance of the section before reinforcement is $M_{Rd} = 59.52$ kN·m. The highest value of the moment on the section under consideration, using the shift rule of moments diagrams, is $M_{Ed} = 17.23$ kN·m. The cross-section between the support and the considered cross-section can transfer loads also without the use of FRP strips.

2.2. Design calculations for serviceability limit state (SLS)

Serviceability limit state (SLS) verification is carried out to deflections, cracking and stresses with the same basic assumption and load conditions as for unstrengthened slab. To perform verifications at the SLS it is necessary to evaluate the position of the neutral axis of the transformed section, as well as the value of the moment of inertia under both the cracked and uncracked conditions prior to and after installation of FRP strengthening system.

2.2.1. Stress condition

To include the influence of initial strain is made the following assumption:

$$\frac{\varepsilon_{c0}}{\varepsilon_c'} = \frac{M_{0k}}{M_{k,rc}} \cdot \frac{h - x_0}{x_{rc}} \tag{2.59}$$

The depth of neutral axis after FRP application is calculated from static moment equilibrium:

$$\frac{1}{2bx_{rc}^2} + \left(\alpha_{s,\text{eff}} - 1\right) \cdot A_{s2} = \alpha_{s,\text{eff}} A_{s1} \cdot (d - x_{rc}) + \alpha_{f,\text{eff}} A_f \cdot \left(h - \left(1 + \frac{\varepsilon_{c0}}{\varepsilon_c'}\right) x_{rc}\right) \tag{2.60}$$

The above equation can be transformed to quadratic equation in form $Ax^2 + Bx + C = 0$:

$$A = 1/2B \tag{2.61}$$

$$B = (\alpha_{s,\text{eff}} - 1) \cdot A_{s2} + \alpha_{s,\text{eff}} A_{s1} + \alpha_{f,\text{eff}} A_f \tag{2.62}$$

$$C = -(\alpha_{s,\text{eff}} - 1) \cdot A_{s2} a_{s2} - \alpha_{s,\text{eff}} A_{s1} d - \alpha_{f,\text{eff}} A_f h + \alpha_{f,\text{eff}} A_f \frac{M_{0k}}{M_{k,rc}} \cdot (h - x_0) \tag{2.63}$$

$$\Delta = B^2 - 4AC \tag{2.64}$$

$$x_{rc} = \frac{-B + \sqrt{\Delta}}{2A} = 64.10\ mm \tag{2.65}$$

$$\varepsilon_c' = \varepsilon_{c0} \frac{M_{k,rc}}{M_{0k}} \cdot \frac{x_{rc}}{h - x_0} = 0.00108 \tag{2.66}$$

Stress limitations are established according to:

$$\sigma_c = E_{c,\text{eff}} \varepsilon_c' = 11.71 \text{ MPa} < \sigma_{c\lim} = 0.6 f_{ck} = 21 \text{ MPa} \tag{2.67}$$

$$\varepsilon_{s1} = \varepsilon_c' \frac{d - x_{rc}}{x_{rc}} = 0.00145 \tag{2.68}$$

$$\sigma_{s1} = E_s \varepsilon_{s1} = 290.66 \text{ MPa} < \sigma_{s\lim} = 0.8 f_{yk} = 320 \text{ MPa} \tag{2.69}$$

$$\varepsilon_f = \varepsilon_c' \frac{h - x_{rc}}{x_{rc}} - \varepsilon_{c0f} = 0.00080 \tag{2.70}$$

$$\sigma_f = E_f \varepsilon_f = 127.49 \text{ MPa} < \sigma_{f\lim} = 0.8 f_{fuk} = 2000 \text{ MPa} \tag{2.71}$$

$$\sigma_f = E_f \varepsilon_f = 127.49 \text{ MPa} < \sigma_{f\lim} = 0.8 f_{yk} \frac{E_f}{E_s} = 2000 \text{ MPa} \tag{2.72}$$

Stress conditions are fulfilled.

2.2.2. Crack control (for quasi – permanent load combination, $M_{k,qp}$)

To protect the internal steel reinforcement from corrosion and to guarantee the functionality of the RC member, crack widths should be limited in accordance to the crack width limitations provided in EC2 ($w_{\max} = 0.3$ mm). The crack control is performed according to [1], chapter 7.3.2. The residual service life span in hours is $t = 28$ days (672 h). The cracking develops later than 28 days, so $f_{ct,\text{eff}} = f_{\text{ctm}}$. The calculation of crack width is iterative. It can be used by making an initial assumption for w_k to calculate the the slip of reinforcing steel and FRP, s_s and s_f. It is assumed for iteration $s_s = w_k/2$ and $s_f = w_k/2$. The results presented below are the final results from iteration. To calculate the mean strain in the FRP between cracks it is needed the strain in the FRP reinforcement at the cracked section. The depth of the neutral axis after FRP application is calculated from static moment equilibrium. The static moment equilibrium is transform to quadratic equation in form $Ax^2 + Bx + C = 0$. To include the influence of initial strain is made the corresponding assumption as for stress control, but for $M_{k,qp} = 40.67$ kN·m:

$$\frac{\varepsilon_{c0}}{\varepsilon_c'} = \frac{M_{0k}}{M_{k,qp}} \cdot \frac{h - x_0}{x_{qp}} \tag{2.73}$$

$$1/2bx_{qp}^2 + (\alpha_{s,\text{eff}} - 1) \cdot A_{s2} \cdot (x_{qp} - a_{s2}) = \alpha_{s,\text{eff}} A_{s1} \cdot (d - x_{qp}) + \alpha_{f,\text{eff}} A_f \cdot \left(h - \left(1 + \frac{\varepsilon_{c0}}{\varepsilon_c'} \right) x_{qp} \right) \tag{2.74}$$

$$1/2bx_{qp}^2 + \left[(\alpha_{s,\text{eff}} - 1) \cdot A_{s2} + \alpha_{s,\text{eff}} A_{s1} + \alpha_{f,\text{eff}} A_f \right] x_{qp} - (\alpha_{s,\text{eff}} - 1) \cdot A_{s2} a_{s2} - \alpha_{s,\text{eff}} A_{s1} d - \alpha_{f,\text{eff}} A_f h + \alpha_{f,\text{eff}} A_f \frac{M_{0k}}{M_{k,qp}} \cdot (h - x_0) = 0 \tag{2.75}$$

$$A = 1/2b \tag{2.76}$$

$$B = (\alpha_{s,\text{eff}} - 1) \cdot A_{s2} + \alpha_{s,\text{eff}} A_{s1} + \alpha_{f,\text{eff}} A_f \tag{2.77}$$

$$C = -(\alpha_{s,\text{eff}} - 1) \cdot A_{s2} a_{s2} - \alpha_{s,\text{eff}} A_{s1} d - \alpha_{f,\text{eff}} A_f h + \alpha_{f,\text{eff}} A_f \frac{M_{0k}}{M_{k,qp}} \cdot (h - x_0) \tag{2.78}$$

$$\Delta = B^2 - 4AC \tag{2.79}$$

$$x_{qp} = \frac{-B + \sqrt{\Delta}}{2A} = 63.5 \text{ mm} \tag{2.80}$$

$$\varepsilon_c' = \varepsilon_{c0} \frac{M_{k,qp}}{M_{0k}} \cdot \frac{x_{qp}}{h - x_0} = 0.00093 \tag{2.81}$$

$$\varepsilon_f = \varepsilon_c' \frac{d_f - x_{qp}}{x_{qp}} - \varepsilon_{c0f} = 0.00054 \tag{2.82}$$

The parameters in the bilinear bond law are taken as characteristic values [1], $s_{0k} = 0.20$ mm and $\tau_{b1k} = 4.35$ N/mm^2. The mean bond stress of FRP [1] is calculated according to:

$$s_{1k} = 2.5\frac{50}{E_{cm}}\tau_{b1k} = 0.016 \text{ mm} \tag{2.83}$$

$$\tau_{bm} = \begin{cases} \dfrac{\tau_{b1k}}{2s_{1k}}s_f & \text{for } \ 0 \le s_f \le s_{1k} \\ \dfrac{\tau_{b1k}\left(s_f^2 - 2s_f s_{0k} + s_{1k}s_{0k}\right)}{2s_f\left(s_{1k} - s_{0k}\right)} & \text{for } \ s_{1k} \le s_f \le s_{0k} \end{cases} = 2.45 \text{ N/mm}^2 \tag{2.84}$$

The mean bond stress of internal steel reinforcement for ribbed bars and medium bond conditions ($k_s = 1$, $a_s = 0.25$) is equal to:

$$k_t = (1 + 10t)^{0.08} - 1 = 1.02 \tag{2.85}$$

$$k_{s,\text{eff}} = \frac{1}{(1 + k_t)a_s}k_s = 1.98 \tag{2.86}$$

$$\tau_{sm} = \frac{k_{s,\text{eff}}\sqrt{f}_{cm}}{a_s + 1}s_s^{a_s} = 3.82 \text{ N/mm}^2 \tag{2.87}$$

The effective area of concrete in tension surrounding the steel reinforcement for $x_{II} = 61.2$ mm is calculated according to:

$$h_{c,\text{eff}} = \min\left[2.5(h - d), \frac{d - x_{II}}{3}\frac{h}{2}\right] = 29.6 \text{ mm} \tag{2.88}$$

$$A_{c,\text{eff}} = bh_{c,\text{eff}} = 29601 \text{ mm}^2 \tag{2.89}$$

The bond coefficient referring to the difference in bond behaviour derived from the boundary conditions of the single crack state, $k_{fb} = 4$ is equal:

$$\xi_f = \sqrt{\frac{\tau_{bm}E_s\phi_s}{\tau_{sm}k_{fb}E_f t_f}} = 1.64 \tag{2.90}$$

The strain ratio referred to respective axial stiffness of the external and the internal reinforcement is:

$$\delta_f = \frac{2\xi_f^2}{\xi_f^2 + 1} = 1.46 \tag{2.91}$$

$$\eta_f = \frac{(1 + E_f A_f/E_s A_s)\delta_f}{1 + (E_f A_f/E_s A_s)\delta_f} = 1.34 \tag{2.92}$$

The maximum crack spacing is calculated as follows:

$$s_{r,\max} = \frac{f_{ct,\text{eff}}A_{c,\text{eff}}}{2\tau_{bm}}\frac{k_{fb}E_f t_f\xi_f^2}{E_s A_s + E_f A_f\xi_f^2} = 100.71 \text{ mm} \tag{2.93}$$

The mean strain in the concrete between cracks is calculated as follows:

$$\varepsilon_{cm} = 0.4\frac{f_{ct,\text{eff}}}{E_{cm}} = 0.000038 \tag{2.94}$$

The mean strain in the FRP between cracks equals to:

$$\varepsilon_{fm} = \varepsilon_f \eta_f - 0.5 f_{ct,\text{eff}} A_{c,\text{eff}} \left(\frac{\xi_f^2}{E_s A_s + E_f A_f \xi_f^2} \right) = 0.00040 \tag{2.95}$$

The upper characteristic value of the theoretical crack width in RC members strengthened with externally bonded with FRP laminates based on the finial iteration equals:

$$w_k = s_{r,\max} \left(\varepsilon_{fm} - \varepsilon_{cm} \right) = 0.037 \text{ mm} \tag{2.96}$$

That means that crack control condition is fulfilled: $w_k = 0.037$ mm $< w_{\max} = 0.3$ mm

2.2.3. Long-term deflection (for quasi – permanent load combination, $M_{k,qp}$)

Depth of the neutral axis after FRP application is calculated as: $x_{qp} = 63.5$ mm. The moment of inertia for uncracking and cracking section before strengthening are $I_1 = 610347205$ mm^4, $I_2 = 256070880$ mm^4, respectively. The moment of inertia for strengthening section is:

$$I_{2f} = bx_{qp}^3/3 + (\alpha_{s,\text{eff}} - 1) \cdot A_{s2} \cdot (x_{qp} - a_{s2})^2 + \alpha_{s,\text{eff}} A_{s1} \cdot (d - x_{qp})^2 + \alpha_{f,\text{eff}} A_f \cdot (h - x_{qp})^2 = 333149081 \text{ mm}^4 \tag{2.97}$$

The considered slab is simply supported and distributed loading, so $\alpha_M = 5/48$. The coefficient taking influence of the duration of the loading is equal to $\beta = 0.5$, for sustained loads. The deflections before and after strengthening are as follows:

$$I_{2f} = bx_{qp}^3/3 + (\alpha_{s,\text{eff}} - 1) \cdot A_{s2} \cdot (x_{qp} - a_{s2})^2 + \alpha_{s,\text{eff}} A_{s1} \cdot (d - x_{qp})^2 + \alpha_{f,\text{eff}} A_f \cdot (h - x_{qp})^2 = 333149081 \text{ mm}^4 \tag{2.98}$$

$$a_I = \alpha_M \frac{M_{k,qp} l^2}{E_{c,\text{eff}} I_1} = 22.4 \text{ mm} \tag{2.99}$$

$$a_{II0} = \alpha_M \frac{M_{0k} l^2}{E_{c,\text{eff}} I_2} = 36.6 \text{ mm} \tag{2.100}$$

$$a_{II\Delta M} = \alpha_M \frac{(M_{k,qp} - M_{0k}) l^2}{E_{c,\text{eff}} I_{2f}} = 12.8 \text{ mm} \tag{2.101}$$

$$h_{cr} = h - x_I = 87.5 \text{ mm} \tag{2.102}$$

$$M_{cr} = \frac{f_{\text{ctm}} I_I}{h_{cr}} = 22.39 \text{ kN} \cdot \text{m/m} \tag{2.103}$$

$$\zeta = 1 - \beta \left(\frac{M_{cr}}{M_{k,qp}} \right)^2 = 0.85 \tag{2.104}$$

$$a = \zeta(a_{II0} + a_{II\Delta M}) + (1 - \zeta) a_I = 45.3 \text{ mm} \tag{2.105}$$

The deflection doesn't meet the required condition and the slab needs strengthening, $a = 45.3$ mm $> a_{\text{per}} = 23.6$ mm. The number of CFRP laminates (11 laminates), which fulfilled the above condition is not possible to use in presented elements. To reduce deflection to the limit value the prestressed CFRP EA laminates should be used.

3. Conclusions

The paper presents analysis of the ultimate limit state associated with the debonding failure in two critical zones: the support and the span. The more accurate method for intermediate crack debonding is very complex and the calculation must be conducted in more detailed calculation program (that needs iteration). In publication [1] the main attention was drawn to the relatively large uncertainty typically observed on the prediction of the crack spacing. In the presented example for the end debonding analysis also the force equilibrium in section is obtained iteratively. However, for the analysis of flexural crack closest to the point of zero moment, approximate formulas may be used to determine force in the section. In the intermediate crack debonding analysis the ratios $\Delta F_{fEd}/\Delta F_{fRd}$ are from 0.01 to 0.08, depending on the cross-section. For comparison in simplified analysis of (simplified FRP stress method in which the strain and stress in the FRP is limited, not describe in this paper) the ratio M_{Ed}/M_{Rd} is equal 0.76. The same rule of comparison the presented above method for the end plate debonding, the analysis gives ratio $M_{Ed}/M_{Rd}(l_b) = 0.44$ (end anchorage at the flexural crack closest to the point of zero moment) and $F_{fEd}/F_{fbd} = 0.20$ (the analysis at an arbitrary element between cracks). It is clear visible that the methods requiring more computational effort give lower values of comparing to the simplified method that makes these methods economically more beneficial. Based on the serviceability limit state (SLS) the crack control (for quasi – permanent load combination, $M_{k,qp}$) is fulfilled, however the long-term deflection does not fulfil the required deflection.

References

[1] *FIB Bulletin 90 – Externally applied FRP reinforcement for concrete structures*. FIB, 2019.

[2] R. Niedermeier, "Gemischte Bewehrung bei klebearmierten Bauteilen", in *Münchner Massivbau-Seminar 1997*.

[3] U. Neubauer, *Verbundtragverhalten geklebter Lamellen aus Kohlenstofffaserverbundwerkstoff zur Verstärkung von Betonbauteilen*. Institute of Building Materials, Concrete Construction & Fire Protection, Braunschweig TU, 2000, doi: 10.24355/dbbs.084-201304241329-0.

[4] R. Niedermeier and K. Zilch, "Zugkraftdeckung bei klebearmierten Bauteilen", *Beton- und Stahlbetonbau*, vol. 96, no. 12, 2001, doi: 10.1002/best.200101000.

[5] K. Zilch, R. Niedermeier, and W. Finckh, *DAfStb-Heft 592: Praxisgerechte Bemessungsansätze für das wirtschaftliche Verstärken von Betonbauteilen mit geklebter Bewehrung – Verbundtragfähigkeit unter statischer Belastung*. Berlin, 2012.

[6] K. Zilch, R. Niedermeier, and W. Finckh, *Strengthening of concrete structures with adhesive bonded reinforcement: design and dimensioning of CFRP laminates and steel plates*. Berlin: Ernst & Sohn, 2014.

[7] PN-EN 1992-1-1:2008 Eurokod 2: Projektowanie konstrukcji z betonu – Część 1-1: Reguły ogólne i reguły dla budynków. PKN, 2008.

[8] PN-EN 1990:2004 Eurokod: Podstawy projektowania konstrukcji. PKN, 2004.

Wzmocnienie na zginanie na podstawie fib Bulletin 90

Słowa kluczowe: zewnętrzne wzmocnienie na zginanie (EBR), materiały kompozytowe (FRP), zginanie, wzmacnianie, nośność

Streszczenie:

Wzmacnianie elementów żelbetowych na zginanie przy użyciu taśm i mat kompozytowych jest powszechnie stosowaną metodą zwiększania nośności. Potrzeba zwiększenia nośności może wynikać ze zmiany funkcji użytkowej obiektu, jak również z powstania dodatkowego obciążenia skupionego lub liniowego na stropie. Taki przykład jest podstawą niniejszego artykułu, w którym zaprezentowano projektowanie wzmocnienia płyty na zginanie przy użyciu taśm węglowych (Carbon Fiber Reinforced Polymer – CFRP), według wytycznych fib Bulletin 90 w wersji dokładnej. Analizie poddano płytę żelbetową wzmocnioną 3 taśmami na 1 metr szerokości płyty. Dodatkowe obciążenie wynikało z zaprojektowania nowej ściany. W pierwszym kroku obliczenia zostały wykonane w odniesieniu do możliwości odspojenia taśmy w części środkowej. Ze względu na symetrię analizowano tylko połowę płyty, rozpoczynając położenie kolejnych przekrojów od środka belki. Metoda dokładna opiera się na analizie naprężeń przyczepności taśm CFRP do betonu na odcinkach między rysami. Warunek nośności jest spełniony, jeśli siła rozciągająca w taśmach CFRP ΔF_{fEd} jest niższa niż siła przyczepności taśm do betonu ΔF_{fRd} na każdym odcinku pomiędzy rysami: $\Delta F_{fEd} \leq \Delta F_{fRd}$. Siła występująca w taśmach CFRP w miejscach, gdzie założono położenie kolejnych rys została ustalona iteracyjnie na podstawie równowagi przekrojów. W przedstawionym przykładzie warunek ten został spełniony w każdym analizowanym przekroju. Następnie wykonano obliczenia odnoszące się do możliwości odspojenia taśmy w miejscu zakotwienia. W wersji uproszczonej tej analizy należy wykazać, że moment wynikający z działających obciążeń M_{Ed} jest mniejszy niż moment $M_{Rd}(l_b)$ obliczony zgodnie z wytycznymi fib Bulletin 90. Wersja dokładna, czyli analiza odspojenia końca taśmy pomiędzy rysami może być konieczna w elementach, w których z powodu niskiej wytrzymałości betonu na rozciąganie rysa od zginania bliska miejscu zerowego momentu powstanie bardzo blisko podpory. Siła rozciągająca w taśmach CFRP F_{fEd} na ostatnim odcinku między rysami powinna być mniejsza niż siła przyczepności kompozytu do betonu: F_{fbd}, $F_{fEd} \leq F_{fbd}$. Obliczenia wykonane według metody dokładnej i uproszczonej wykazały, że zaproponowane wzmocnienie jest wystarczające. W przedstawionym elemencie problematyczne okazało się spełnienie wymagań stanu granicznego użytkowalności związanych z ograniczeniem ugięć. Zgodnie z zaleceniami fib Bulletin 90 sprawdzono wartość naprężeń występujących w taśmach CFRP, stali oraz betonie i wykazano, że są one mniejsze niż dopuszczalne. Wykonano obliczenia szerokości rozwarcia rys również uzyskując spełnienie warunku $w_k = 0,037$ mm $< w_{\max} = 0,3$ mm. Jednak otrzymana wartość ugięcia $a = 45,3$ mm znacznie przewyższa wartość dopuszczalną $a_{\text{per}} = 23,6$ mm. Liczba taśm CFRP, która pozwoliłaby na spełnienie warunku związanego z ugięciami elementu jest niemożliwa do zastosowania w rozważanym przykładzie. Rozwiązaniem tego problemu mogłoby być zastosowanie taśm sprężonych. Podsumowując, prezentowane metody weryfikacji nośności na zginanie wymagają znacznego wysiłku obliczeniowego. Na podstawie analizy w miejscu zakotwienia widoczne jest wprost, że metoda dokładna pozwala na projektowanie bardziej ekonomiczne. Jednak ostatecznie stanem granicznym decydującym o ilości zastosowanych do wzmocnienia taśm okazał się nie stan graniczny nośności, a stan graniczny użytkowalności, którego spełnienie okazało się niemożliwe przy zastosowaniu taśm biernych.

Received: 2023-08-01, Revised: 2023-09-22